



Gallium Nitride Nanocrystal Spectroscopic Properties using Diamondoids Structures

Bilal K. Al-Rawi

Department of Physics, College of Education for Pure Sciences, University of Anbar, Anbar, Iraq.

Received: 23 Nov 2017

Revised: 13 Dec 2017

Accepted: 03 Jan 2018

*Address for correspondence

Bilal K. Al-Rawi

Department of Physics,
College of Education for Pure Sciences,
University of Anbar, Anbar, Iraq.
E.mail: bilal_al_rawi@yahoo.com



This is an Open Access Journal / article distributed under the terms of the **Creative Commons Attribution License (CC BY-NC-ND 3.0)** which permits unrestricted use, distribution, and reproduction in any medium, provided the original work is properly cited. All rights reserved.

ABSTRACT

In the current work, we study the electronic structure, Fourier Transform Infrared (FTIR), and Raman spectra of GaN diamondoids as a function of particle size and shape, using density functional theory (DFT). We calculated the vibrational spectra of GaN and analyzed them with respect to mass, force constant, and intensity of vibration. Since the size and shape of diamondoids vary among the nanoparticles, we compared them using the tetrahedral angles and bond lengths.

The results show that the bond length strongly depends on the shape of the diamondoid molecules. The bond length was also found to increase as the number of cages increased. The total energy as well as the energy gap decrease as the size of nanocrystal clusters increases. These trends might persist at the level of bulk properties because surface effects are negligible in diamondoids.

Keywords: GaN, diamondoids structures, infrared spectroscopy, Raman spectra, nanocrystal cluster, DFT.

INTRODUCTION

GaN is a group III-nitride and a semiconductor [1]. It is a hard compound that exhibits two crystal structures: zinc-blende and wurtzite. In the zinc-blende structure, GaN has a wide band gap of 3.46 eV, which makes it useful for optoelectronic applications such as light-emitting diodes (LEDs) and other light emitting devices [2,3]. In addition, the nanocrystals of GaN are used in nanoscale electronics and biochemical sensing [4]. This is because these nanocrystals help us maneuver many physical properties that are required for electronic devices, such as energy gap and lattice constant. Similarly, the recently discovered higher diamondoids (octamantane) have generated excitement



**Bilal Al-Rawi**

for their potential as nanoscale devices. However, these devices are based on molecular electronics, in which diamondoids are isolated on metal surfaces. The properties of such systems are not yet fully understood [5].

THEORY

We investigated the properties of GaN diamondoids using ab-initio DFT. This method involves full geometrical optimization in accordance with the Hartree-Fock method (HF), which is one of the most accurate methods to simulate the electronic structure and study the optical properties of nanocrystals. Even though this method is computationally expensive, in terms of memory and time, it was feasible at our computational facility [6]. All the calculations of geometrical optimization were executed by combining ab-initio DFT with the generalized gradient approximation (GGA) proposed by Perdew, Burke, and Ernzerhof (PBE), in the program Gauss View 5.0 according with Gaussian 09W [7].

To perform these calculations, the basis function 3-21G was chosen so that all the vibrational analyses could be performed at the same theoretical level. Using this program, the stable positions of atoms in the nanocrystal were determined and the vibrational frequencies and Raman lines of GaN nanocrystals were calculated [8].

Diamondoids are carbon nanostructures that have a perfect size and selectable shapes along with passivated hydrogen and sp³-hybridized. Being perfectly size-selectable, they are well suited to investigate the size-dependence of electronic structure, i.e., quantum confinement (QC) effects [9]. To study these effects, using the current method, GaN diamondoids were constructed from the size of a few molecules to the nano region (bottom-up method). At every intermediate size, we calculated the vibrational frequencies to understand their variation as a function of the size of GaN clusters [10].

RESULTS AND DISCUSSION

GaussView 5.0 and Gaussian 09W were used to optimize the geometries and calculate the vibrational spectra of GaN diamondoid nanocrystals (diamantane, tetramantane, hexamantane, and octamantane). The calculated frequency error that results from ab-initio calculations [11].

The present scale factor is one of the nearest scale factors of the unscaled data (very close to 1) and thus was used without modification for all spectra. The geometrical optimization method was used in the present work to obtain the electronic structure of GaN molecules, while the infrared spectrum is shown as a function of frequency (Figure 1). These include cage-like molecules such as diamantane Ga₇N₇H₂₀, tetramantane Ga₁₁N₁₁H₂₈, hexamantane Ga₁₃N₁₃H₃₀, octamantane Ga₂₀N₂₀H₄₂.

Bulk GaN is identified by its IR absorption at approximately 0–700 cm⁻¹ vibrational mode peak [12].

However, the highest intensity line in for GaN diamantane was seen at 706.45 cm⁻¹ while octamantane was seen at 1885.21 cm⁻¹. We noticed a shift in the intensity maxima toward the right side of the infrared vibrational frequencies. This includes the 997–2495 cm⁻¹ modes in the Ga-H and N-H vibrational regions. The region around the broad peak at 706 cm⁻¹ is indicative of Ga–N.

(Figure 2) shows the highest intensity line in the present calculation for GaN diamantane is at 1711.36 cm⁻¹, for tetramantane it is at 1788.96 cm⁻¹ and for hexamantane it is at 1799.79 cm⁻¹ while for octamantane it is at 2288.92 cm⁻¹. A shift in the intensity maxima at about 3500 cm⁻¹ of the Raman vibrational frequencies was noted. This includes the 1543–3489 cm⁻¹ modes in the Ga-H and N-H vibrational regions.





Bilal Al-Rawi

Equation (1) relates the frequency of vibration to the harmonic force constant and reduced mass [13]:

$$\nu = \frac{1}{2\pi} \sqrt{\frac{k}{\mu}} \quad (1)$$

The reduced mass μ of two particles of masses m_a and m_b is given by [14]:

$$\frac{1}{\mu} = \frac{1}{m_a} + \frac{1}{m_b} \quad (2)$$

Although the above equation is for diatomic molecules, it can also be used to explain the vibrational modes of other larger molecules.

Represents the reduced masses of GaN-diamondoid vibrations, the left parts of Ga-N vibrations are larger than the right parts of H vibrations and the right part is nearly equal to 1 shown in (Figure 3). The high reduced mass mode (HRMM) of octamantane is larger than of the other diamondoids.

(Figure 4) shows GaN-diamondoid force constants as a function of vibration frequency. As deduced from a part of the statistical difference between the numbers of vibration frequencies of all GaN-diamondoids, all shapes as shown (Figure 4) are nearly similar and begin from approximately 0 cm^{-1} of Ga-N vibrations and ends at less than 300 cm^{-1} , whereas right parts of H vibrations start at approximately 375 cm^{-1} and ends at nearly 2180 cm^{-1} .

The GaN diamondoid bond lengths generally increase as the number of cages increases with a remarkable dependence on the size of the diamondoid molecules. The experimental bulk of GaN bond lengths (19.5 nm) is inside this distribution range, as shown in (Figure 5).

(Figure 6) shows a comparison between the density of tetrahedral angles in GaN-diamantane and GaN-octamantane. In a piece of bulk far from the surface all tetrahedral angles should have the value 109.47° [15]. As we can see from (Figure 6A) the highest peak of GaN-diamantane is at 106° while that of GaN-octamantane in (Figure 6B) is at 110°. The tetrahedral angle of octamantane is much closer to the ideal value 109.47° than that of diamantane. This is due to the effect of surface reconstruction that has an effect on all the atoms in GaN-diamantane (all the atoms are bonded to surface hydrogen atoms) while it has an effect on some of the atoms in GaN-octamantane.

(Figure 7) shows the tetrahedral angle as a function of the number of cages for GaN. The variation of the tetrahedral angle between atoms starts from gallium hydrogenated surface layer (H-Ga-N angle) and reach the nitride hydrogenated surface layer (Ga-N-H angle) at the opposite face of the nanocrystal. The tetrahedral angles range from 109.47° is compared with the tetrahedral angle if an ideal diamond and zincblende structure. Tetrahedral angles approach the value of bulk as we go to higher diamondoids. This angle takes oscillatory values starting from gallium terminated surface and ending at the nitride terminated surface. The tetrahedral angle of octamantane is much closer to the ideal value 109.47° than that of diamantane.

This is due to the effect of surface reconstruction that has an effect on all the atoms in GaN-diamantane (all the atoms are bonded to surface hydrogen atoms), while it has an effect on some of the atoms in GaN-octamantane.

The dihedral angles should have one of the values -180°, -60°, 60° and 180° in bulk zincblende structure [16]. While this might be true for the angles -180° and 180° in GaN-diamantane in (Figure 8A) it is not completely true for the



**Bilal Al-Rawi**

angles -60° and 60° . For GaN-octamantane (Figure 8B) the situation improves for the angles -60° and 60° that become closer to its ideal value.

The comparison between the pulsed depolarization spectrum in GaN-diamantane and GaN-octamantane shown in Figure 9. GaN is used in a semiconductor for pulsed power applications, switching several megawatts of electrical power in several nanoseconds [17]. As a sensor material, GaN is able to work reliably in conditions where other materials may malfunction.

The energy gap reduces from 3.69 eV in GaN-diamantane to 3.39 eV in GaN-octamantane. This reduction is in compliance with the confinement effects that require size reduction of the energy gap as manifested in (Figure10). The value of energy gap for GaN-experimental is more similar to the bulk value at 3.46 eV.

(Figure11) shows the variation in the total energy with the varying number of GaN atoms. It shows that the total energy decreases with increasing the number of Ga and N atoms. On the scale shown in this figure, the size dependence of the energy is linear.

CONCLUSION

As concluding remarks, we can note that the present theory can adequately reproduce most of the experimental data of infrared vibrational frequencies. This includes the $997\text{--}2495\text{ cm}^{-1}$ modes in the Ga-H and N-H vibrational region. The region of Ga-N mode of vibration is between $0\text{--}700\text{ cm}^{-1}$. The present theory suggests different types of Ga-H and N-H vibrations, which include symmetric, antisymmetric, wagging, scissor, rocking, and twisting modes. It also reproduces the movement of the highest reduced mass of Ga-N of nanocrystals while growing in size.

REFERENCES

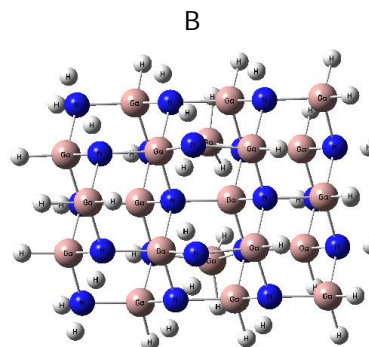
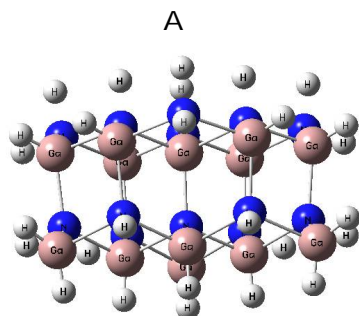
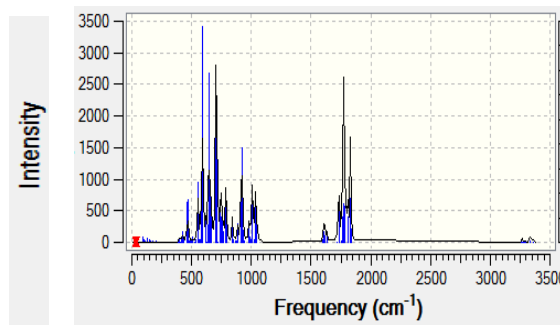
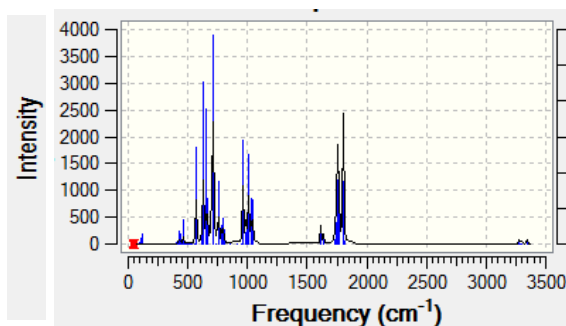
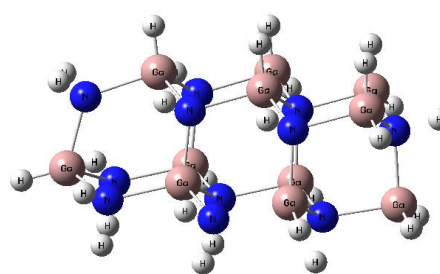
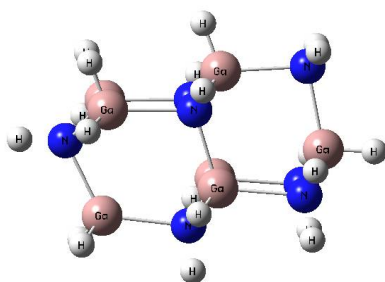
1. S. Strite and H. Morkoç, Journal of Vacuum Science & Technology B: Microelectronics and Nanometer Structures Processing, Measurement, and Phenomena, GaN, AlN, and InN: A review., 1992, Volume 10, Issue 4, 1237.
2. A. I. Hochbaum, R. Chen, R. Diaz Delgado, W. Liang, E. C. Garnett, M. Najarian, A. Majumdar and P. Yang, Enhanced thermoelectric performance of rough silicon nanowires, 2008, PubMed, Nature 451, 163.
3. J. Ristic, E. Calleja, S. Fernandez-Garrido, L. Cerutti, A. Trampert, U. Jahn and K. H. Ploog, J. Cryst, On the mechanisms of spontaneous growth of III-nitride nanocolumns by plasma-assisted molecular beam epitaxy Growth, Journal of Crystal Growth, ELSEVIER, 2008, Volume 310, Issue 18, Pages 4035-4045.
4. R. Koester, J. S. Hwang, C. Durand, D. Le Si Dang and J. Eymery, Self-assembled growth of catalyst-free GaN wires by metal-organic vapour phase epitaxy, PubMed, Nanotechnology 21, 2010, 015602.
5. J. B. Baxtera and E. S. Aydil, Dye-sensitized solar cells based on semiconductor morphologies with ZnO nanowires, Solar Energy Materials and Solar Cells, ELSEVIER, 2006, Volume.90, Issue5, Pages 607-622.
6. J. B. Foresman and A. E. Frisch, Exploring Chemistry with Electronic Structure Methods: A Guide to using Gaussian, Gaussian, 1996, 2nd edition, Gyan Books Pvt. Ltd.
7. M. J. Frisch, G. W. Trucks and H. B. Schlegel, Gaussian 03 Revision B-01, Gaussian, 2003, Inc, Pittsburgh, PA, USA.
8. N.N. Greenwood, Spectroscopic properties of inorganic and organometallic compounds, Royal Society of Chemistry, 1976, Volume 9.
9. Tobias Z. , Robert R. , Andre K. , Andrey A., Tetyana V. , Lesya V. , Pavel A., Peter R., Thomas M. ,1 and Torbjorn R. Exploring covalently bonded diamondoid particles with valence photoelectron spectroscopy, The Journal of Chemical Physics, 2013, Volume 139, Issue 8139.





Bilal Al-Rawi

10. Anil K. Kandalam, Ravindra Pandey, M. A. Blanco, Aurora Costales, J. M. Recio and John M. Newsam, First Principles Study of Polyatomic Clusters of AlN, GaN, and InN. 1. Structure, Stability, Vibrations, and Ionization, J. Phys. Chem. B 2000, 104, 2000, 4361-4367.
11. Yuyu Wang, Emmanouil Kioupakis, Xinghua Lu, Daniel Wegner, Ryan Yamachika, Jeremy E. Dahl, Robert M K Carlson, Steven G. Louie, Michael F. Crommie, Spatially resolved electronic and vibronic properties of single diamondoids molecules, nature materials, 2008, volume 7 , pp.38-42.
12. T. Azuhata, T. Sota, K. Suzuki, S. Nakamura [J. of Physics: Condensed Matter, (UK) 1995, Volume7, p. L129-33].
13. Thornton, Stephen T.; Marion, Jerry B. Classical Dynamics of Particles and Systems (5th ed.), 2003, Brooks Cole.
14. J.R. Forshaw, A.G. Smith, Dynamics and Relativity, Wiley, 2009.
15. Nasir H N, Abdulsattar M A, Abduljalil H M, Electronic Structure of Hydrogenated and Surface Modified GaAs Nanocrystals: Ab Initio Calculations, Adv. Condens. Matter, 2012, Phys., 348-354.
16. Alice Qinhua Zhou, Corey S. O'Hern, Lynne Regan, The Power of Hard-Sphere Models: Explaining Side-Chain Dihedral Angle Distributions of Thr and Val, Biophysical journal, 2012, Volume 102, Issue 10, p2345-2352.
17. Aldo Mele, Anna Giardini, Tonia M. Di Palma, Chiara Flamini, Hideo Okabe and Roberto Teghil. Preparation of the group III nitride thin films AlN, GaN, InN by direct and reactive pulsed laser ablation, International Journal Of Photoenergy, 2001, Vol.3, p111-121.





Bilal Al-Rawi

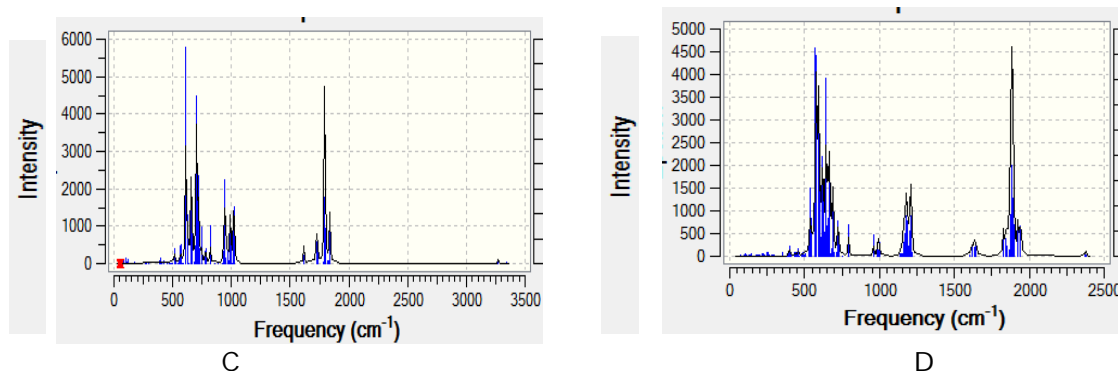


Figure 1: Shape of Geometrically Optimized and IR Spectra of GaN-Diamondoids as a Function of Frequency of :A- Diamantanediamantane $Ga_7N_7H_{20}$ B- Tetramantane $Ga_{11}N_{11}H_{28}$ C- Hexamantane $Ga_{13}N_{13}H_{30}$ D- Octamantane $Ga_{20}N_{20}H_{42}$.

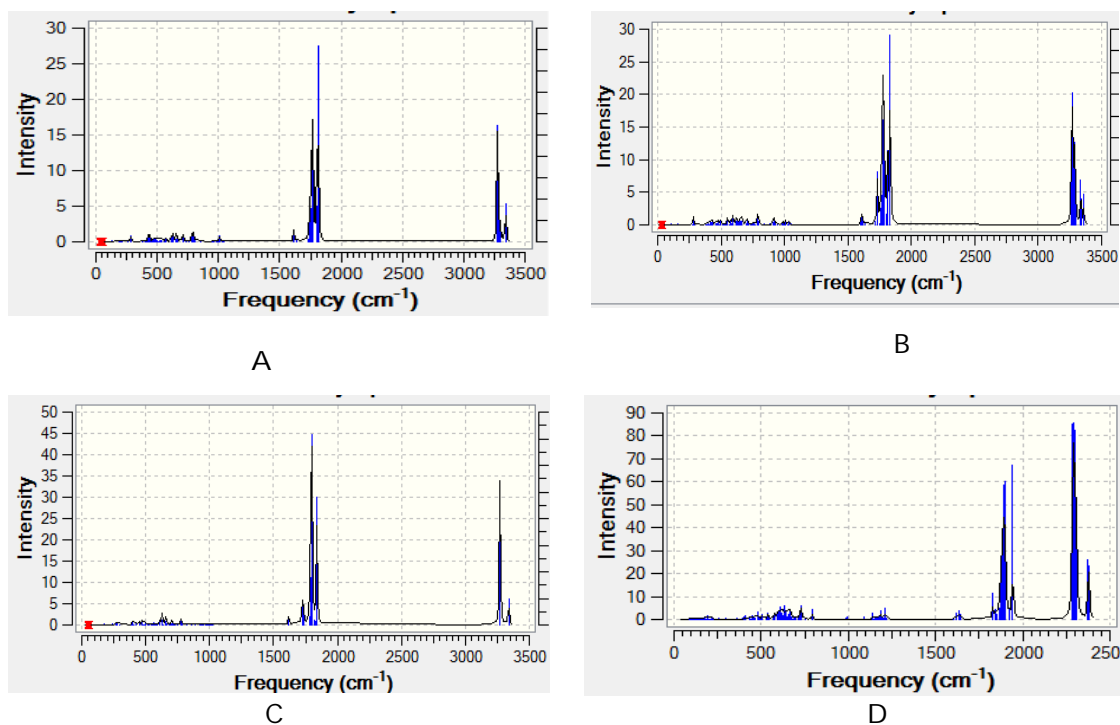


Figure 2: Raman Intensities of GaN-Diamondoids of Infrared Spectrum as a Function of Frequency of A- Diamantanediamantane $Ga_7N_7H_{20}$ B- Tetramantane $Ga_{11}N_{11}H_{28}$ C- Hexamantane $Ga_{13}N_{13}H_{30}$ D- Octamantane $Ga_{20}N_{20}H_{42}$.





Bilal Al-Rawi

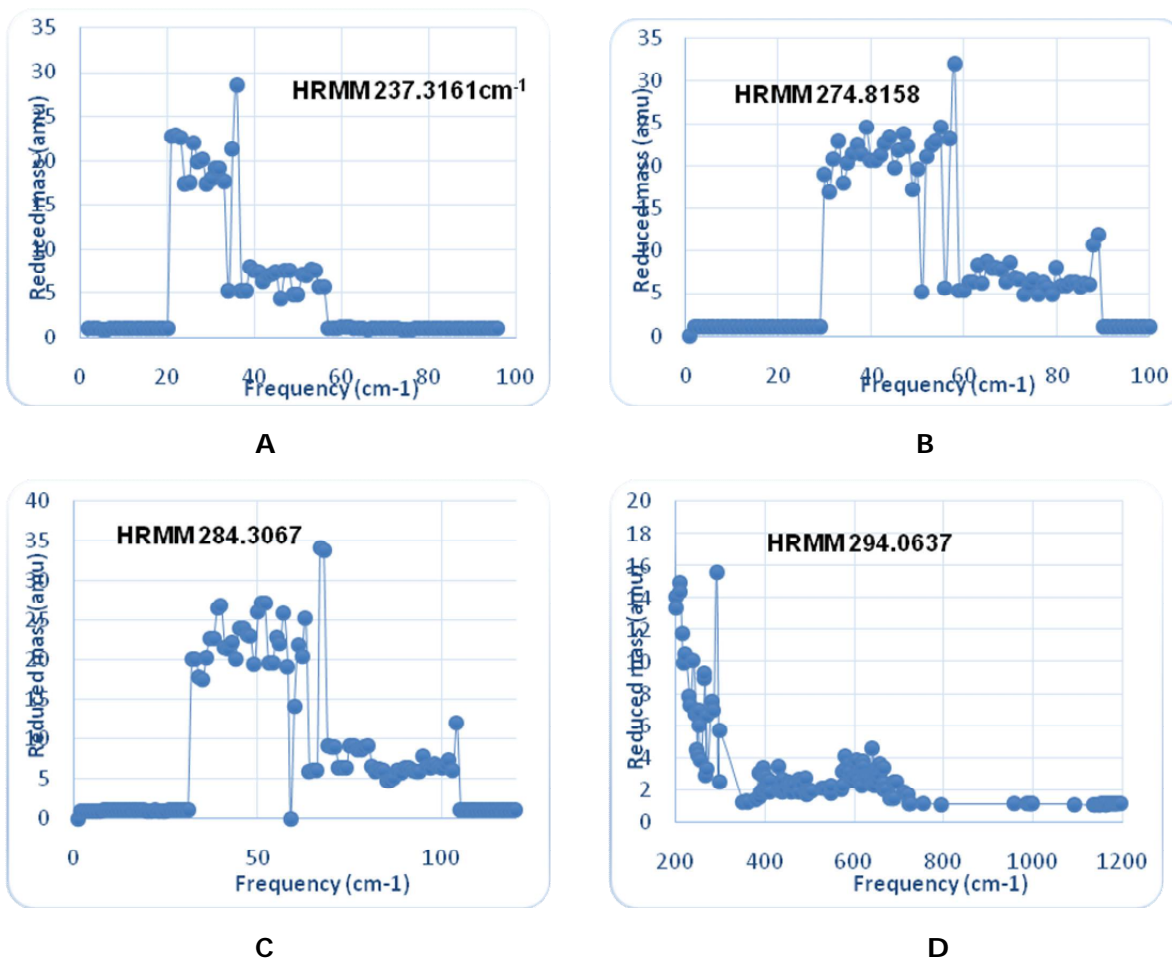
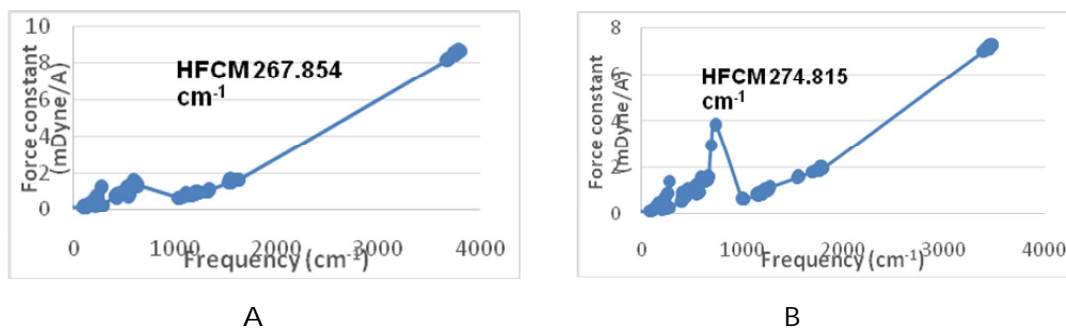


Figure 3: GaN-Diamondoids reduced mass as a function of vibration frequency of A. Diamantanediamantane $Ga_7N_7H_{20}$ B- Tetramantane $Ga_{11}N_{11}H_{28}$ C- Hexamantane $Ga_{13}N_{13}H_{30}$ D- Octamantane $Ga_{20}N_{20}H_{42}$.





Bilal Al-Rawi

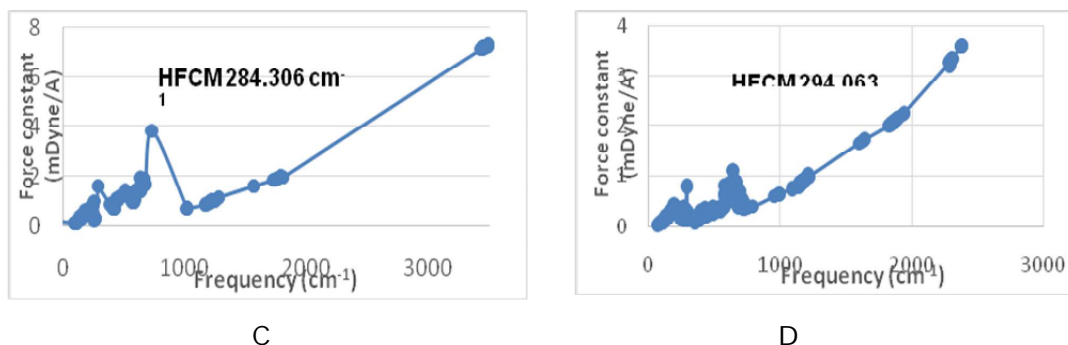


Figure 4: Force Constant of GaN- Diamondoids as a function of frequency of A. Diamantanediamantane $Ga_7N_7H_{20}$ B- Tetramantane $Ga_{11}N_{11}H_{28}$ C- Hexamantane $Ga_{13}N_{13}H_{30}$ D- Octamantane $Ga_{20}N_{20}H_{42}$

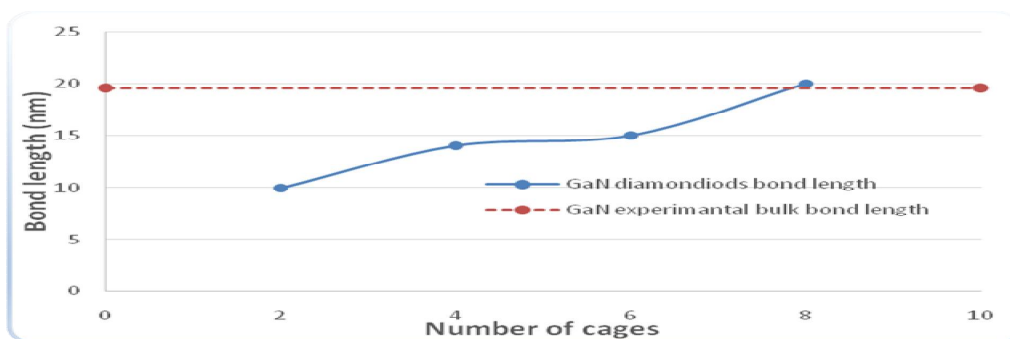


Figure 5: Bond lengths of GaN Diamondoids .PBE/3-21G theory is used for the calculations of this figure. The dashed line represents the experimental bulk value of Ga-N bond length.

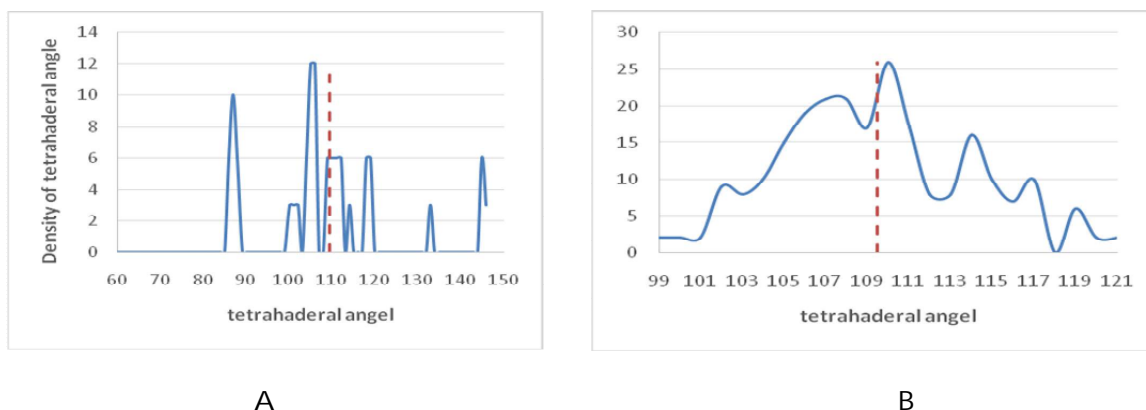


Figure 6: (A) Density of Tetrahedral Angles in GaN-diamantane and (B) Density of Tetrahedral Angles in GaN-octamantane. The dashed line represents the ideal value of Zincblende Structure Experimental at 109.47° [13].





Bilal Al-Rawi

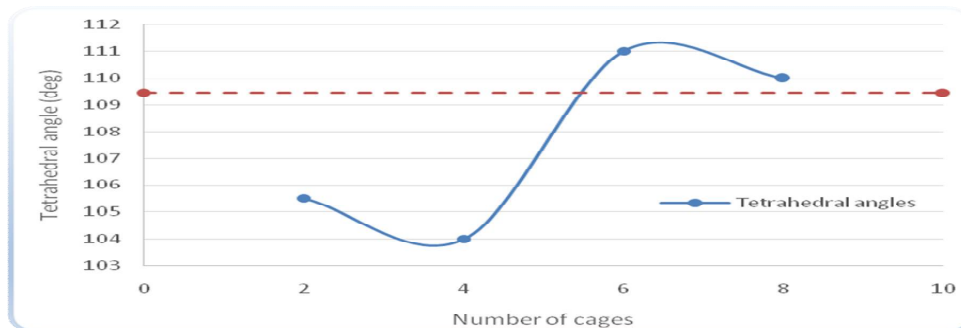


Figure 7: The variation of Tetrahedral Angle as a function of number of cages for GaN. This angle is compared with the Experimental Ideal Diamond and Zincblende Structure Tetrahedral Angle of 109.47°

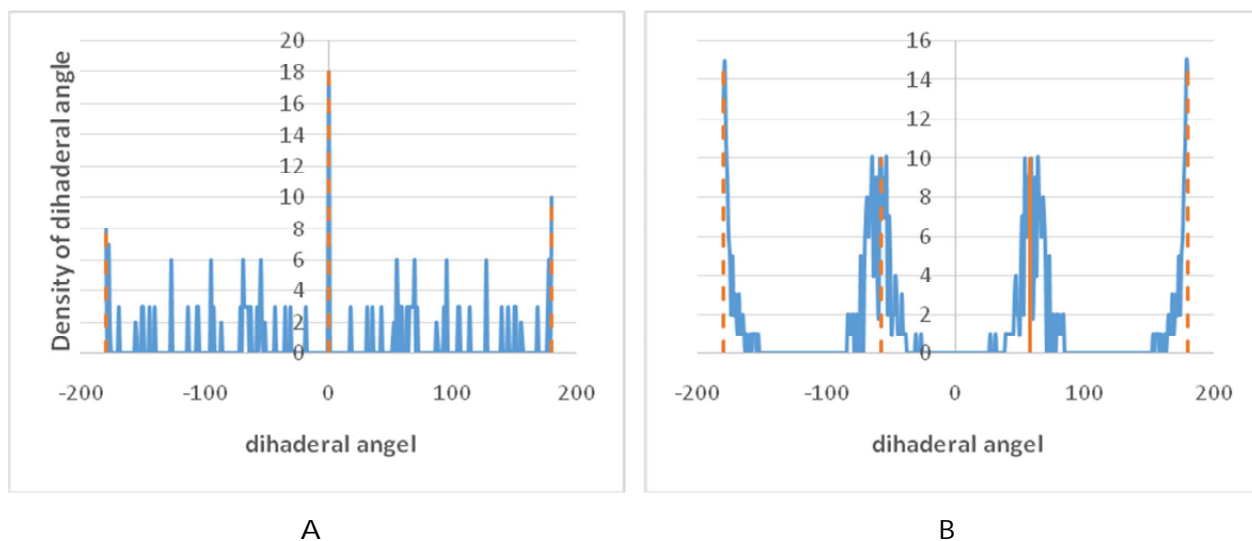
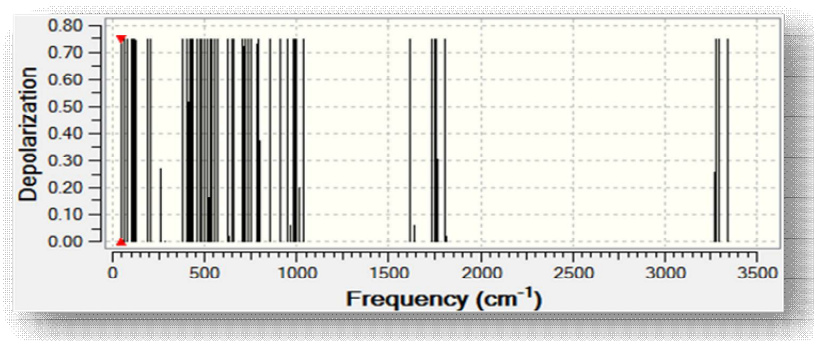


Figure 8: A) Density of Dihedral Angles in GaN-diamantane and B) Density of Dihedral Angles in GaN-Octamantane. Dashed lines show the experimental ideal value of this angle in bulk Zincblende Crystals i.e. $\pm 60^\circ$ or $\pm 180^\circ$ [16].





Bilal Al-Rawi

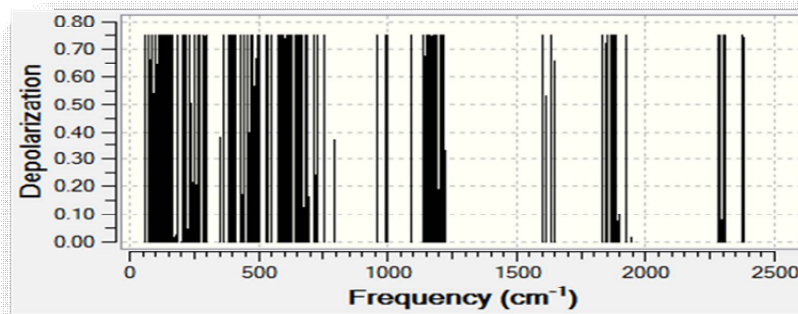


Figure 9: The Comparison between the pulsed Depolarization Spectrums in (a) GaN-Diamantane and (b) GaN-Octamantane.

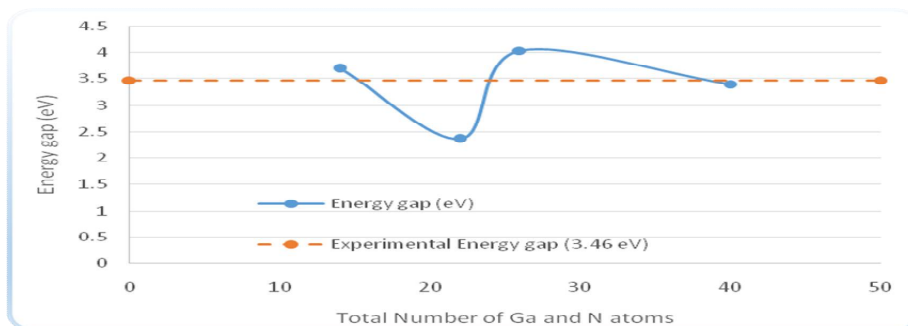


Figure 10: Energy Gap as a function of total number of Ga and N Atoms in GaN Diamondoids. The dashed line represents the experimental value of bulk GaN gap at 3.46 (eV).

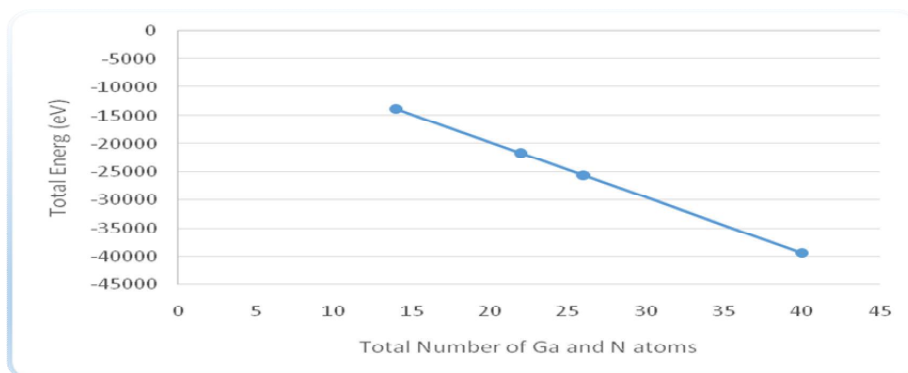


Figure 11: Total energy as a function of total number of Ga and N Atoms in GaN Diamondoids.

